Velocity Measurements of Particles in the Impeller of a Centrifugal Slurry Pump

J R. Kadambi [(1)] , M. Mehta [(2)],
Mechanical and Aerospace Engineering department,
Case Western Reserve University, Cleveland, Ohio. 44106 U.S.A.

J. Sankovic [(3)]
NASA Glenn Research Center, Cleveland, Ohio 44135, U.S.A

G. Addie [(4)], R. Visintainer [(5)]
GIW Industries, Grovetown, Ga. 30813, U.S.A.

[(1)]E-Mail: jaikrishnan.kadambi@case.edu
[(2)]E-Mail: Mehul.Mehta@Trans.ge.com
[(3)]E-Mail: John.M.Sankovic@nasa.gov
[(4)]E-Mail: gaddie@giwindustries.com
[(5)]E-Mail: RVisintainer@giwindustries.com

ABSTRACT

Particle Image Velocimetry (PIV) is successfully utilized for investigation of slurry flow in the impeller of a centrifugal slurry pump. The slurry pump is equipped with optically clear casing and impeller. The slurry is made up of sodium-iodide solution (NaI) solution and 500 micron glass beads. The refractive indices of the NaI solution and the casing and impeller material (acrylic) are matched to facilitate the PIV measurements inside the impeller. A slight mismatch of refractive index between the NaI solution and glass beads facilitates the measurements of particle velocities. Figure 1 shows the optically clear centrifugal slurry pump. The experiments are conducted at speeds of 1000 and 750 rpm and for different blade position. Particle volumetric concentration of 1, 2 and 3% are used. The PIV images are analyzed using the cross correlation technique. The velocity of the particles were obtained. The particle velocities obtained are an average of 1000 image pairs. Relative velocity plots show that flow separation takes place on the suction side of the blade in the region below the blade tip for clear fluid flow conditions. This was expected as the pump is made to operate with slurry and not a single-phase liquid. At higher pump speeds and particle volumetric concentrations, a marked improvement in the slurry flow in the impeller is observed i.e., the recirculation zone decreases. This results from the centrifugal forces on the particles and its inertia at that speed. Also the slurry particles are pushed on the pressure side of the blade and slide on it which can result in frictional wear. The results of these tests are presented in this paper.

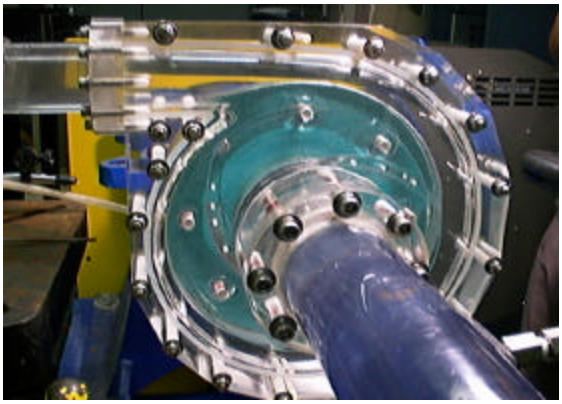

Figure 1: Centrifugal slurry pump with clear casing and clear impeller.

INTRODUCTION

Solid-liquid slurries are transported over short and medium distances via pipelines in many mining, industrial, and fossil-energy related processes. The centrifugal slurry pump, a critical component of such a slurry transport system encounters some of the most erosive environment, resulting in high wear and short life. Wear inside the pump casing is a function of the operating conditions, the geometry of the casing collector and the wear resisting properties of the material. To predict the erosion, one requires the knowledge of the two-phase flow field, so that the wear coefficients (Roco and Addie, 1987, Tuzson et al., 1998, Pagalthivarthi et al., 1992) can be determined experimentally. Intrusive measurement methods compromise the two phase flow field by disturbing the flow; therefore, non-intrusive techniques are the preferred method to study the flow behavior. Non-intrusive measuring techniques include acoustic ultrasound, magnetic resonance imaging, X-ray tomography, neutron radiography, particle image velocimetry (PIV), laser Doppler velocimetry (LDV), Phase Doppler Interferometry, the Malvern Laser Diffraction measurement technique and holographic interferometry. A detailed literature survey is provided by Mehta (2004).

Thomas et al. (1986) conducted tests to locate the streamlines, stagnation point and areas of separation around the tongue region of a slurry pump. The slurry pump was made from plexiglass. The flow visualization experiments were carried out by injecting the air bubbles in the flow. Paone et al (1988) used Particle Displacement Velocimetry (PDV) to measure the flow field in a diffuser of a centrifugal pump with clear Plexiglas® casing and impeller. Experiments were performed with water as the fluid and metallic coated micro spheres (diameter 4 μm, density 2.6 g/cm^3) as seed particles. They identified the blade wake path. Dong et al. (1992a, 1992b) used PDV technique to visualize the flow inside the volute of a centrifugal pump. Neutrally buoyant particles of 30 μm mean diameter were used as seed and it was observed that although most of the blade effects occur near the impeller tip, they are not limited to this region. In addition they stated that the entire flux pulsating within the volute reaches a maximum when the blade lines up with the tip of the tongue. LDA measurements were obtained by Cader et al. (1994) in a centrifugal slurry pump using a concentration of 1%. Micron size tracers and 0.8 mm glass beads were used. Fluctuations in angular velocity up to 20%, radial velocity up to 90% and axial velocity up to 200% from their mean velocity components over various impeller angular positions were observed.

A numerical model was developed by Roco and Addie (1983) to obtain velocity, concentration and erosion wear in the casing of a centrifugal slurry pump. Empirical parameters, e.g. slip factor of the impeller and the experimental ratio of erosion rate for the model were obtained from the available experimental data. Other studies of solid-liquid slurry flow in centrifugal pumps and pipelines include Roco et al. (1984, 1985 and 1986), Wilson et al. (1986, 1992 and 1997), Shook and Roco (1991) and Addie (1996).

Kadambi et al. (2000) developed a refractive index matched slurry pump loop to investigate slurry flow in pumps using PIV and presented single phase flow results. Schilling et al. (2001) have conducted numerical simulations to investigate the time dependent 3D turbulent flows through a slurry pump. They start with the flow investigation in 2D and 3D flow without the solid phase, and then 2D transient calculations were compared with the Frozen Rotor approach. Then they performed 3D Frozen Rotor calculations on a slurry pump and compared the results with the measurements. They concluded that the wear zones were found at the leading edge as well as at the suction side of the blade.

Charoenngam et al. (2002, 2003) conducted experiments in a slurry pump using 500 micron glass beads at volumetric concentrations of 2.5% and 5% to study flow in the tongue region. It was observed that in the impeller passage region, the highest velocities were generated on the suction side of the blade and in the blade trailing edge region. Also, the directional impingement mechanism was considered to be more significant at the pressure side of the blade and it was an important parameter with the increase in the speed. This flow loop and PIV technique are used in this study n which the flow field inside the impeller are investigated.

EXPERIMENTAL SET-UP

Slurry Pump Loop Facility

The slurry pump loop facility (developed by GIW Industries, Inc.) used in this investigations is located in the Laser Flow Diagnostics Laboratory, Case Western Reserve University, Cleveland, Ohio, U.S.A. It consists of 50.8 mm I.D. tubing

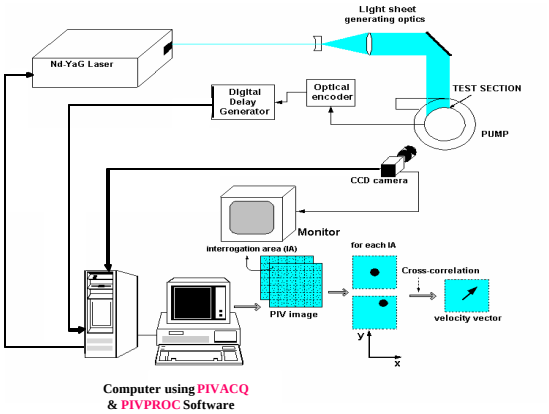

Figure 2: The PIV setup

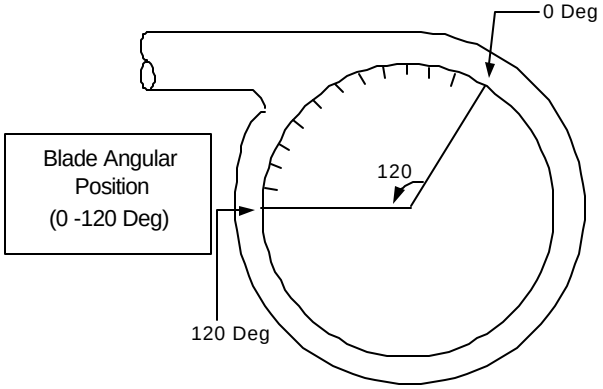

Figure 3: Blade angular position.

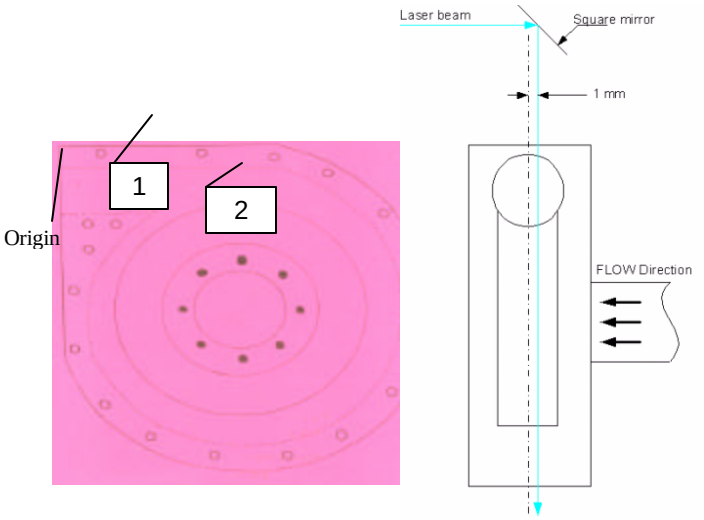

Figure 4: (a) The FOV location. (b) Laser light sheet plane location

closed loop. A 2.1 meter long, 75 mm I.D. PVC straight section upstream of the pump inlet provides a swirl free inlet flow to the pump. In order to minimize particle deposition and unnecessary pump head loss in the system, there are no sharp sudden flow area changes. The flow in the loop is delivered by an optically clear centrifugal slurry pump.

The Optically Clear Centrifugal Slurry Pump

The single stage radially split centrifugal pump was specially designed to provide optical access. The casing of the pump and the impeller are made from optically transparent acrylic (Figure 1). The ratio of pump casing inlet diameter to the discharge diameter is 2.35.The single- or end-suction impeller with shroud on both sides to enclose the liquid passages was installed in a semi volute casing, specially designed for slurry handling. The impeller has three blades. The ratio of the impeller diameter to the eye tip diameter is 2.49.

PIV System

The PIV hardware consists of a 50 mJ/pulse Nd:YAG laser (532 nm wavelength), laser light sheet optics, a CCD camera (Redlake ES 1.0 cross-correlation camera; resolution: 1008 x 1018 pixels) equipped with a 60 mm Micro Nikkor lens (Nikon) and a data acquisition system consisting of a PC and a PIXCI D2X frame grabber card (EPIX) . The laser beam is formed into a 0.2 mm thick light sheet using a combination of cylindrical and spherical lenses. The CCD camera is mounted on a 3-D traverse with a translation accuracy of ±0.0254 mm in each direction, and has its focal axis perpendicular to the plane of the laser light sheet to acquire flow images. Pair of single exposure image frames is required to enable cross-correlation data processing. The image pair acquisition and processing is done using the PIVACQ and PIVPROC software (Wernet,1999). The image pair acquisition is synchronized to the impeller rotation using a once per rev signal. An optical encoder located at the pump shaft generates a signal when the impeller blade reaches a desired location which then triggers the digital delay generator (DDG). The DDG in turn sends a signal to the data acquisition system, which then fires the laser and acquires the images from the PIV camera. Figure 2 shows the PIV setup. Figure 3 shows the angular location of the blade. The 3 blades of the impeller are placed 120 degrees apart (Counter-clockwise).

RESULTS AND DISCUSSIONS

Tests were conducted using a slurry made up of sodium iodide solution (density 1.65 g/cc) in water and spherical glass particles of diameter 500 µm (density 2.5 g/cc). The refractive indices of the sodium iodide solution and the acrylic casing and impeller of the pump were matched so as to obtain flow images without any optical distortion and minimize the light scattering at the liquid-solid interfaces. The slurry solid volumetric concentrations used were 1%, 2% and 3% (corresponding to 1.5%, 2.9% and 4.2% weight concentrations respectively). Figures 4(a) and 4(b) show regions of interest in the casing and impeller of the centrifugal slurry pump, as well as the laser light sheet plane location. The light sheet is off the center plane by 1 mm to avoid the joint between the two parts of the casing. A Field of View (FOV) of 54 mm by 54 mm was used for all locations. The measurements were conducted at flow rates of 120gal/min (725 rpm) and 170gal/min (1000 rpm). The corresponding Reynolds number (based on the impeller diameter and linear velocity of the impeller tip) were $3.1x10^6$ and $4.3x10^6$, for these two flow rates. The fluid velocities were obtained using sodium iodide (NaI) solution (optically clear with the refractive index of 1.485), seeded with silver coated hollow neutrally buoyant glass beads (15 µm). Spherical glass particles of 500 µm mean diameter (refractive index 1.5) were added to clear sodium iodide solution to obtain the slurry flow. Particles were added in the increasing order of volumetric concentration from 1% to 3%. Only the particle velocities are obtained for the slurry flow. However, for brevity, results of the experiments conducted at Location 2, which is in the impeller-blade region at 1000 rpm are discussed. The particles have a higher density than the liquid (2.5 g/cc vs. 1.65 g/cc); therefore do not follow the liquid and the velocities reported for the slurry flow are the particle velocities. A 1000 pairs of PIV images were used to obtain statistically meaningful velocities. This resulted in uncertainty levels of less than 1.0% for liquid velocity and 4% for the 500 µm glass particle velocities. Details of the experimental procedure and the uncertainty analysis are provided by Mehta (2004).

Location 2 covers an intra-blade region in the impeller of the centrifugal slurry pump (Figure 4a). The absolute velocity distribution is obtained for the particles in this location. Figures 8 and 9 show the absolute velocity plots for this location at blade angular positions of 50° and 55° respectively, at a pump speed of 1000 rpm. The results shown in those figures are for both clear fluid flow conditions (a) as well as slurry flow conditions (b to d). The average particle velocity decreases with the increase in the particle concentration (from 6.9 m/s for 1% vol. concentration to 5.7 m/s for 3% vol. concentration). Maximum velocity is obtained for the clear fluid flow conditions and as expected the particle velocities are small and reduce gradually as the volumetric concentration of the slurry particles is increased from 1% to 3%. This is obviously due to the inertia of the particles. The fluid or particle velocity is maximum at the trailing edge and at the suction side of the blade irrespective of the blade positions and flow conditions and reduces in the regions away from the blade. The particle velocity is lower than the blade tip velocity (13.1 m/s) and hence the particles do not hit the suction surface of the blade. Also at the two angular positions, the maximum velocity region shifts down from the impeller line with the increase in the particle concentration. On the pressure side of the blade, the frictional wear pattern can be caused by the particles that cannot be maintained in the suspension and accumulate into sliding layers. The directional impingement wear mechanism, resulting from the particles with velocities that are slower than the blade velocity, can occur on the pressure side of the blade also.

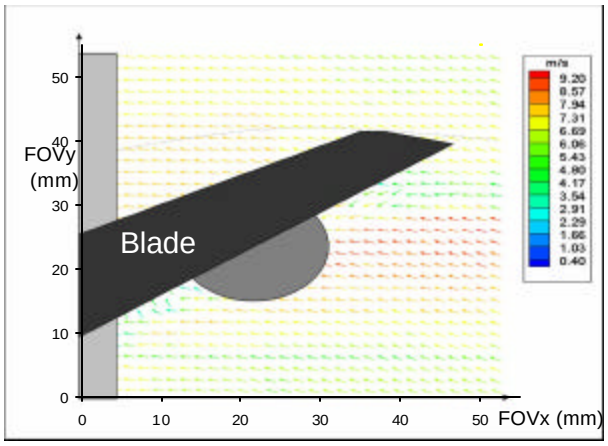

Figure 5(a): Absolute velocity plots at location 2 at 50° blade position and 1000 rpm: Clear Fluid Flow Conditions

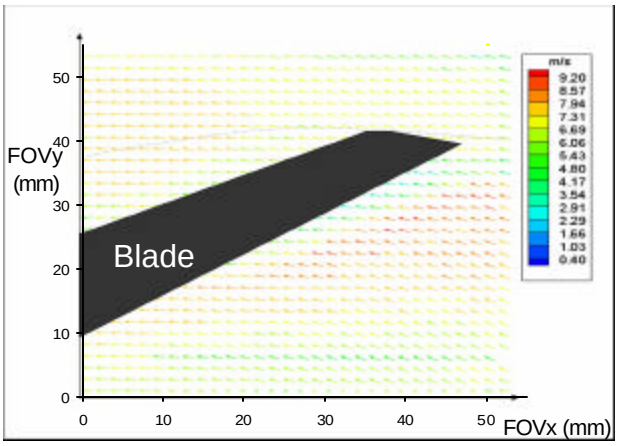

Figure 5(d): Absolute velocity plots at location 2 at 50° blade position and 1000 rpm: 3% Volumetric Concentration

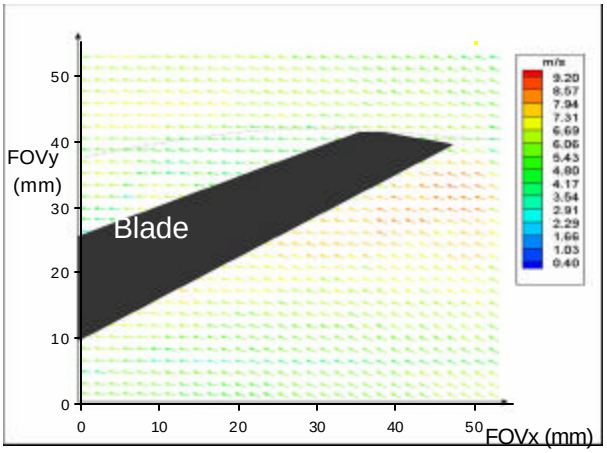

Figure 5(b): Absolute velocity plots at location 2 at 50° blade position and 1000 rpm: 1% Volumetric Concentration

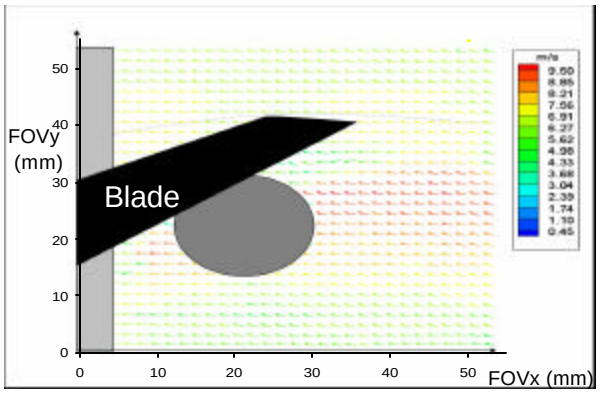

Figure 6(a): Absolute velocity plots at location 2 at 55° blade position and 1000 rpm: Clear Fluid Flow Conditions

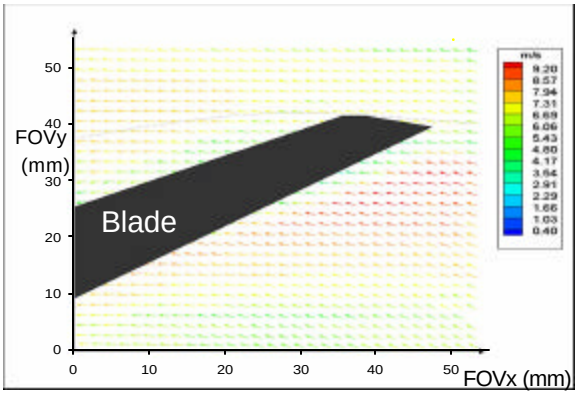

Figure 5(c): Absolute velocity plots at location 2 at 50° blade position and 1000 rpm: 2% Volumetric Concentration

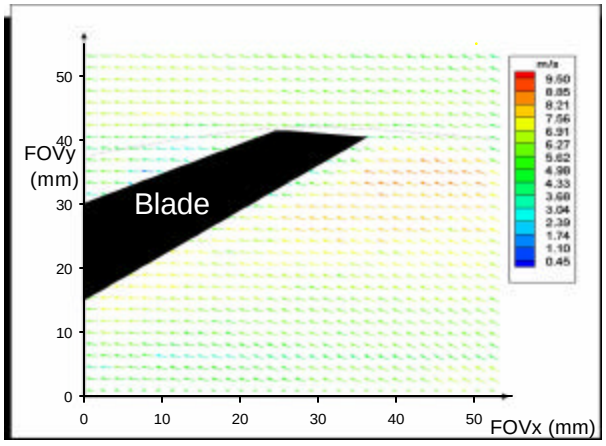

Figure 6(b): Absolute velocity plots at location 2 at 55° blade position and 1000 rpm: 1% Volumetric Concentration

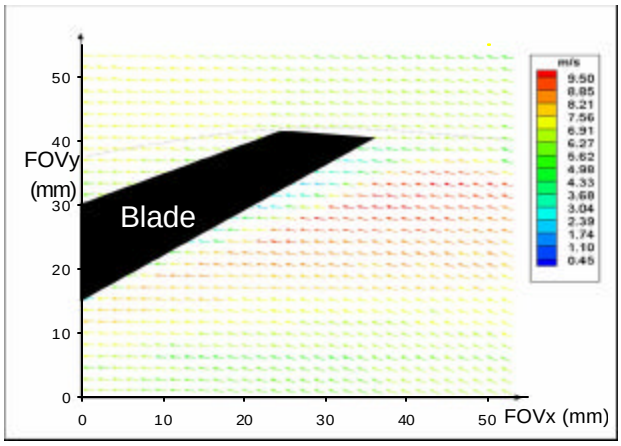

Figure 6(c): Absolute velocity plots at location 2 at 55° blade position and 1000 rpm: 2% Volumetric Concentration

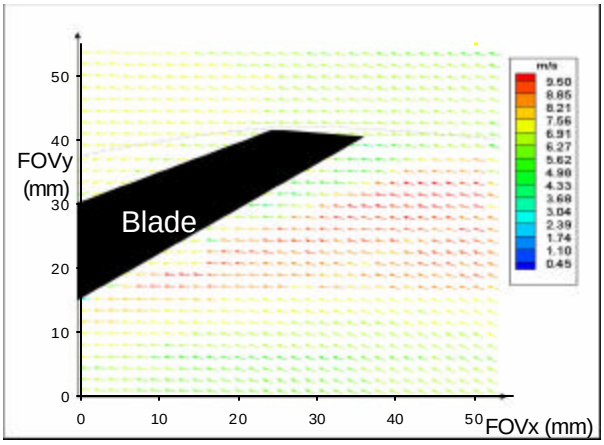

Figure 6(d): Absolute velocity plots at location 2 at 55° blade position and 1000 rpm: 3% Volumetric Concentration

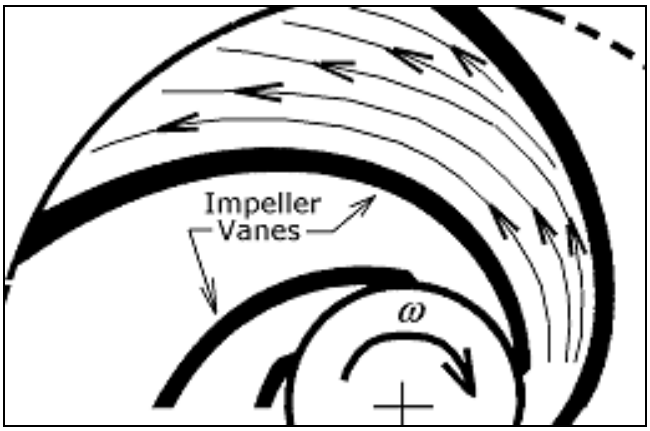

(a)

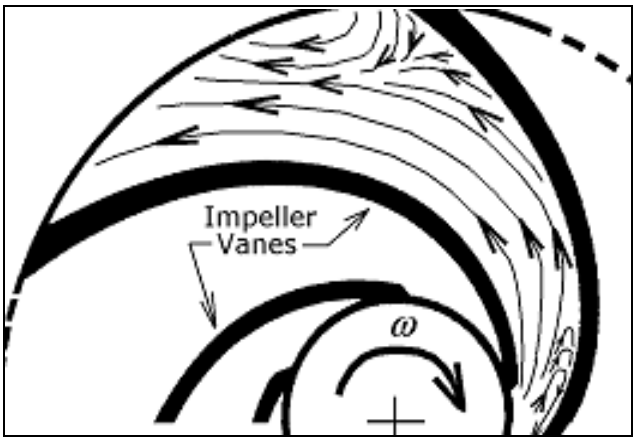

(b)

Figure 7: Flow patterns in the impeller at (a) best efficiency and, b) Flow significantly lower than the best efficiency point [23].

Relative Velocity

The relative velocity, V_{rel}, of the single-phase fluid as well as for the slurry particles inside the impeller were obtained using Equation 1.

$$\vec{V}_{rel} = \vec{V}_{abs} - \vec{V}_{blade} \quad (1)$$

Where, $\vec{V}_{abs}$ is the fluid or particle absolute velocity and $\vec{V}_{blade}$ is the blade velocity. It should be noted that the blade velocity has only the tangential component (equal to rw, where r is the radius and w is the angular velocity). The relative velocities are obtained for single-phase fluid as well as for the flow with the particle volumetric concentrations of 1%, 2% and 3%.

It is important to understand the difference between the slurry pump and the conventional liquid centrifugal pump. In a conventional single phase centrifugal pump, the number of blades is higher, around 6 or 7, the blade passage width is not large and therefore is not prone to the flow separation along the suction surface of the blade as well as recirculation. The flow pattern for flow in a conventional liquid centrifugal pump impeller (Adams, 2003) is shown in Figure 7(a) when the flow is at 100% best efficiency point (BEP). If the pump speeds are lower than the best efficiency point, they become prone to these types of separation and recirculation as shown in Figure 7(b). In slurry pumps, the number of blades is kept to a minimum, normally three as in this case, and as such if used for single-phase flow, one would expect recirculation as shown in Figure 7(b). Figures 11 through 18 show the relative velocities (clear fluid as well as the particles) with respect to the blade for Location 2 (intra-blade region) which covers a substantial portion of the impeller. In these figures coordinate points (0, 0) represent the center of the impeller. Results were obtained at the pump speeds of 725 rpm (Figures from 11 through 14) and 1000 rpm (Figures from 15 through 18) for the clear fluid flow and particle volumetric concentrations of 1%, 2% and 3%. The pump speeds of 725 and 1000 rpm corresponds to 50% and 70% of the design speed. The blade was at 50° position for this analysis. The dotted circular line above the blade in all the figures indicates the impeller shroud line that encloses the blades.

The result shows that with the clear fluid flow conditions for both the pump rpm (Figure 11 and Figure 15), flow separation takes place on the suction side of the blade in the region below the blade tip. For the same flow conditions, the flow moves smoothly along the suction side of the blade depicting a recirculation zone. The intensity of this recirculation zone decreases at the higher concentration of 3% due to particle inertia effects. On the pressure side of the blade the particles are pushed along the blade surface and can result in the frictional wear. The frictional pattern in this case could be a combination of random impingement and direct friction.

At the higher speed of 1000 rpm, which is 70% of BEP, a marked improvement in the slurry flow conditions is observed (Figure 16 through 18). The single-phase flow (Figure 15 5.30) still shows the recirculation and separation. At the BEP speed and higher particle concentration, we believe that the performance for the slurry pump would be further enhanced. The limitations of the pump drive did not allow us to run the pump at higher speeds.

SUMMARY

Particle image velocimetry (PIV) along with refractive index matching technique was successfully used to obtain the velocities of the slurry particles in the impeller of a centrifugal slurry pump. Tests were conducted at speeds of 725 rpm and 1000 rpm using a slurry made up of sodium iodide solution as a working fluid and glass beads (500µm mean diameter)as solid particles at volumetric concentrations of 1%,2%, and 3%.

In the intra blade region of the impeller (Location 2), the highest velocities were obtained on the suction side of the blade and in the blade trailing edge region as the blade sweeps through and its magnitude increases with the increase in the pump speed. But its magnitude was less than that of circumferential velocity of the blade tip. Relative velocity plots show that flow separation takes place on the suction side of the blade in the region below the blade tip for clear fluid flow conditions. This was expected as the pump is made to operate with slurry and not a single-phase liquid. A marked improvement in the slurry flow in the impeller is observed for higher pump speeds and particle volumetric concentrations, i.e., the recirculation zone decreases. This results from the centrifugal forces on the particles and its inertia at that speed. Also the slurry particles are pushed on the pressure side of the blade and slide on it which can result in frictional wear.

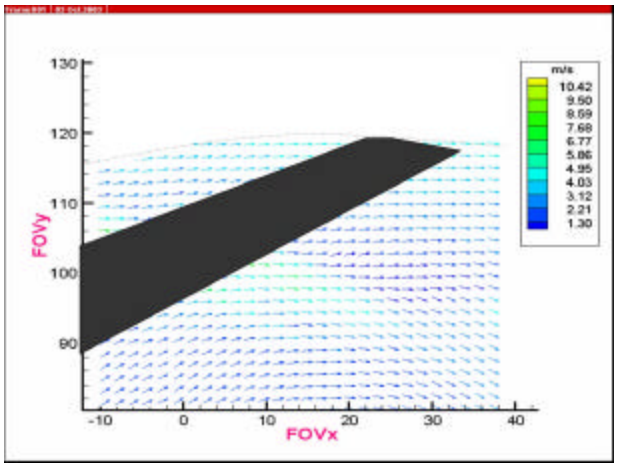

Figure 8: Relative velocity plot at Location 2 (50° blade positions and 725 rpm pump speed) with the clear fluid flow condition.

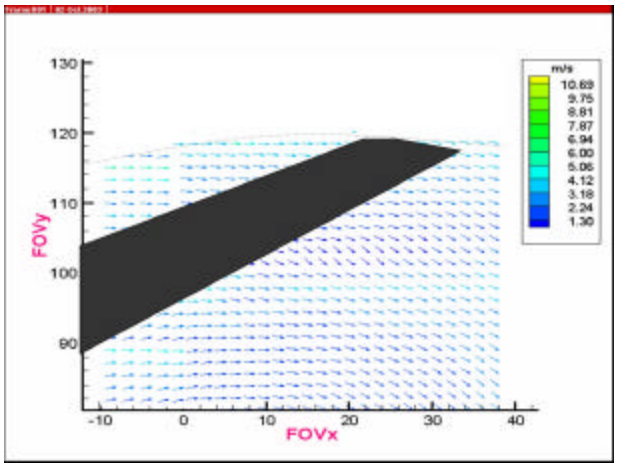

Figure 9: Relative velocity plot at Location 2 (50° blade positions and 725 rpm pump speed) with 1% volumetric concentration of the particles

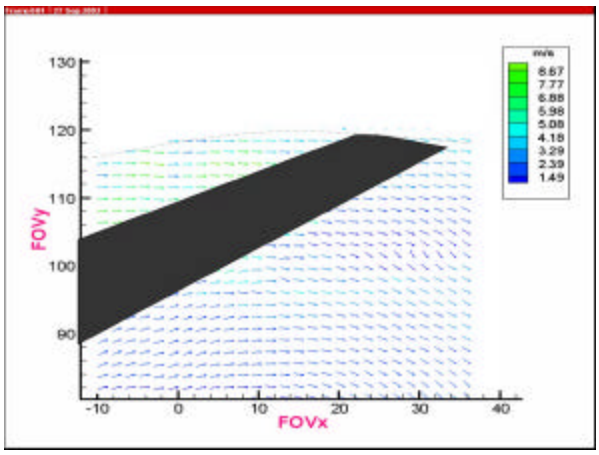

Figure 10: Relative velocity plot at Location 2 (50° blade positions and 725 rpm pump speed) with 2% volumetric concentration of the particles

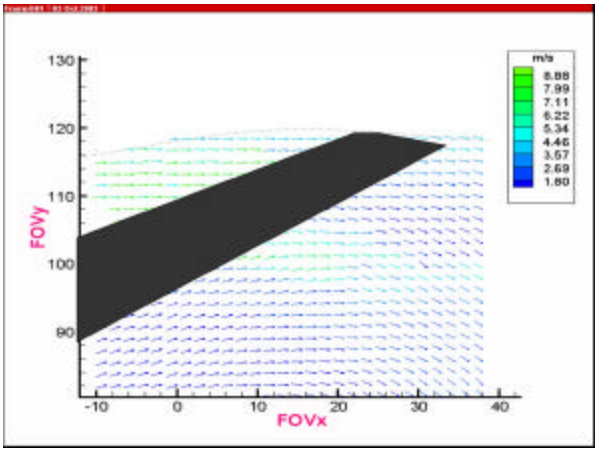

Figure 11: Relative velocity plot at Location 2 (50° blade positions and 725 rpm pump speed) with 3% volumetric concentration of the particles

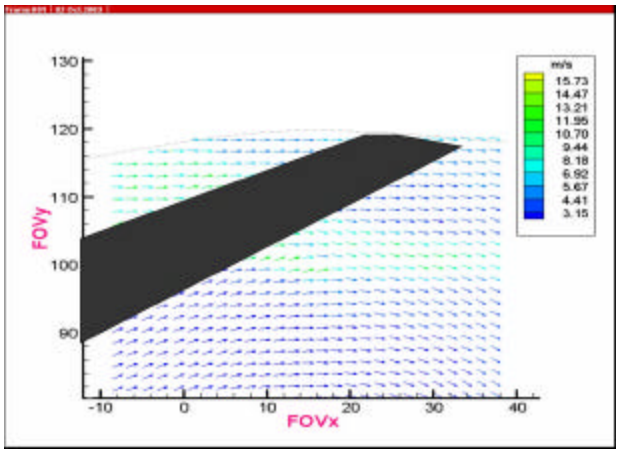

Figure 12: Relative velocity plot at Location 2 (50° blade positions and 1000 rpm pump speed) with clear fluid flow conditions

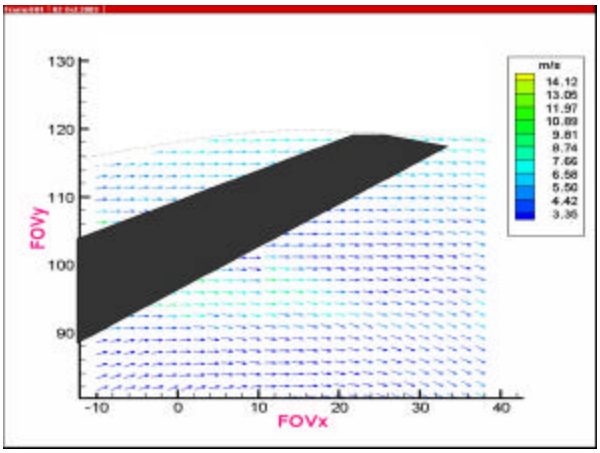

Figure 14: Relative velocity plot at Location 2 (50° blade positions and 1000 rpm pump speed) with 2% volumetric concentration of the particles

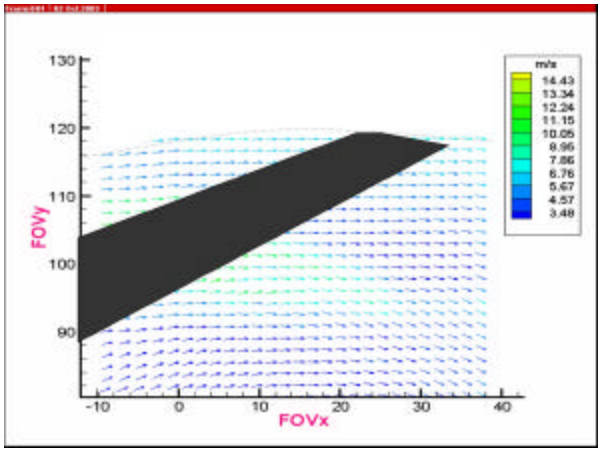

Figure 13: Relative velocity plot at Location 2 (50° blade positions and 1000 rpm pump speed) with 1% volumetric concentration of the particles

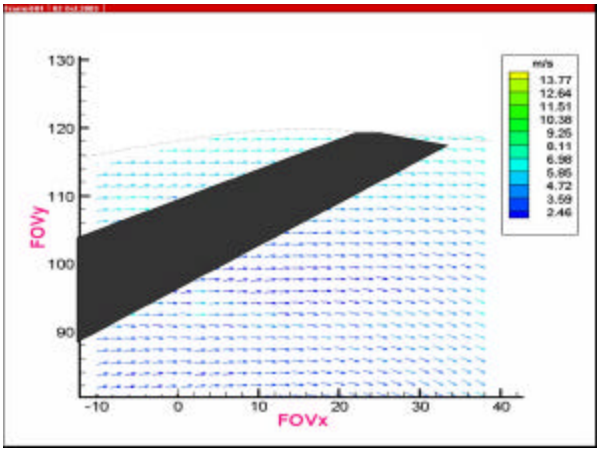

Figure 15: Relative velocity plot at Location 2 (50° blade positions and 1000 rpm pump speed) with 3% volumetric concentration of the particles.

ACKNOWLEDGMENTS

The support provided by GIW Industries Inc., Grovetown, Georgia, U.S.A. is gratefully acknowledged. The support of the Department of Mechanical and Aerospace Engineering at Case Western Reserve University and the NASA Glenn Research Center is also acknowledged. The advise and help of Dr. M. P. Wernet, NASA Glenn Research Center is very much appreciated. The assistance of Mr. D. Conger of the Department of Mechanical and Aerospace Engineering, Case Western Reserve University and Mr. R. Courtwright of GIW industries in making the experimental apparatus operational is greatly appreciated. The assistance of Mr. Venkat Mundla of the Department of Mechanical and Aerospace Engineering at Case Western Reserve University in editing is also acknowledged.

REFERENCES

Adams, M.L., Personal Communications, 2003.

Addie, G. R., 1996. Slurry pipeline design for operation with centrifugal pumps. proceeding of the 13th International Pump Users Symposium, PP 193-210, The Turbomachinery Laboratory, Texas A&M University, Houston, TX, March 1996.

Cader, T., Masbernet, O., and Roco, M. C., 1994. Two-phase velocity distributions and overall performance of a centrifugal slurry pump. *Trans. of ASME, J. Fluids Eng*. vol. 116, pp. 316-323.

Charoenngam, P., Kadambi, J.R., Mehta, M.R., Sankovic, J.M., Wernet, M.P., Addie, G.; " Particulate Velocity Measurements in the Intra-Blade Passages of a Centrifugal Slurry Pump", Proceedings of Fluids Engineering Division Summer Meeting, 4th ASME-JSME Joint Fluids Engineering Conference, Honolulu, Hawaii, July 2003.

Charoenngam, P., Kadambi, J.R., Sankovic, Subramanian, A., J.M., Wernet, M.P., Addie, G., Courtwright, R.; " PIV investigations of Particulate Velocities in the Tongue Region of a Slurry Pump", Proceedings of Fluids Engineering Division Summer Meeting, ASME, Montreal, Canada, July 2002.

Dong, R., Chu, S., and Katz, J., 1992a. Quantitative visualization of the flow within the volute of a centrifugal pump. part a: technique. *Trans. of the ASME*, vol. 114, pp. 390-395.

Dong, R., Chu, S., and Katz, J., 1992b. Quantitative visualization of the flow within the volute of a centrifugal pump. part b: results and analysis. *Trans. of the ASME*, vol. 114, pp. 396-403.

Kadambi, J.R., Addie, G., Subramanian, A., Mahiwan et al., 2000. *"PIV Investigations of Flow in a Centrifugal Slurry Pump"*, 9th International Symposium on Flow Visualization, Edinburgh, Scotland, September 22-26.

Mehta, M.,M.S. Thesis, Mech. and Aero. Eng., Case Western Reserve University, Cleveland, Ohio, 2004.

Pagalthivarthi, K.V. and Helmly, F.W., 1992, "Applications of materials wear testing to solids transport via centrifugal slurry pumps," *Wear Testing of Advanced Materials*, ASTM STP 1167, eds. Divakar, R. and Blau, P.J., pp. 114-126.

Paone, N., Riethmuller, M. L., and Van den Braembussche, R. A., 1988. Application of particle image displacement velocimetry to a centrifugal pump. *4th Intl. Symp. Applications of Laser Techniques to Fluid Mechanics, Lisbon, Portugal*, July 11-14, p. 6.

Roco, M. C. and Addie, G. R., 1983. Analytical model and experimental studies on slurry flow and erosion in pump casings. *8th Intl. Technical Conf. Slurry Transportation, San Francisco, CA.*

Roco, M. C., Addie, G. R., 1987, "Test approach for dense slurry erosion", in *Slurry erosion: uses, application and test methods*, American Soc. for Testing and Materials pp. 185-210.

Roco, M. C., Addie, G. R., Danis, J., and Nair, P., 1984. Modeling erosion wear in centrifugal pumps. *9th Intl. Conf. Hydraulic Transport of Solids in Pipes*, pp. 291-316.

Roco, M. C., Addie, G. R., and Visintainer, R., 1985. Study on casing performances in centrifugal slurry pumps. *Part. Science and Technol*., vol. 3, pp. 65-88.

Roco, M. C., Addie, G. R., Visintainer, R., and Ray, L., 1986. Optimum wearing high efficiency design of phosphate slurry pumps. *Proc. 11th Intl. Conf. Slurry Technology*.

Schilling, R., Maurer, W., Frobenius, M., Addie, G., Muller, T.; "Numerical Simulation of a 3D Flow Field through a Slurry Pump", 4th International Conference on Multiphase Flow, New Orleans, LA, May 2001.

Shook, C. and Roco, M., *Slurry flow: Principles and practice*. Butterworth-Heinemann, ISBN 0-7506-9110-7, Stoneham, MA 02180, 1991.

Thomas, R.N., Kostrzewsky, G.J., Flack, R.D.; "Velocity Measurements in a Pump Volute with a Non-Rotating Impeller", International Journal of Heat and Fluid Flow, Vol.7, No.1, PP 11-20, 1986.

Tuzson, J.J. and Clark, H.Mcl., 1998, "The slurry erosion process in the Coriolis wear tester," *Proc. FEDSM '98, ASME Fluids Engg., Division Summer Meeting, June 21-25, 1998*, Washington, D.C., paper no. FEDSM98-5144.

Wernet, M. P., 1999,'Fuzzy logic enhanced digital PIV processing software', 18th International Congress on Instrumentation for Aerospace Simulation Facilities, (ICIASF), Toulouse, France.

Wilson, K. C., 1986. Effect of solid concentration on deposit velocity. *J. Pipelines*, vol. 5, pp. 251-257.

Wilson, K. C., Addie, G. R., and Clift, R., 1992. *Slurry transport using centrifugal pumps.* Elsevier Science Publishers Ltd.

Wilson, K. C., Addie, G. R., Sellgren, A., and Clift, R., 1997. *Slurry Transport Using Centrifugal Pumps.* 2 Ed: Blackie Academic and Professional.